Switching the ferroelectric polarization in the $S=1/2$ chain cuprate LiCuVO$_4$ by external magnetic fields

F. Schrettle,[1] S. Krohns,[1] P. Lunkenheimer,[1,*] J. Hemberger,[1,†] N. Büttgen,[1] H.-A. Krug von Nidda,[1] A. V. Prokofiev,[2] and A. Loidl[1]

[1]*Experimental Physics V, Center for Electronic Correlations and Magnetism, University of Augsburg, 86135 Augsburg, Germany*
[2]*Institut für Festkörperphysik, Technische Universität Wien, 1040 Wien, Austria*

We present a detailed study of the complex dielectric constant and the ferroelectric polarization in multiferroic LiCuVO$_4$ as function of temperature and external magnetic field. In zero external magnetic field, a spiral spin order with an **ab** helix and a propagation vector along the crystallographic **b** direction is established, which induces ferroelectric order with spontaneous polarization parallel to **a**. The direction of the helix can be reoriented by an external magnetic field and allows switching of the spontaneous polarization. We find a strong dependence of the absolute value of the polarization for different orientations of the spiral plane. Above 7.5 T, LiCuVO$_4$ reveals collinear spin order and remains paraelectric for all field directions. Thus, this system is ideally suited to check the symmetry relations for spiral magnets as predicted theoretically. The strong coupling of ferroelectric and magnetic order is documented and the complex (H,T) phase diagram is fully explored.

I. INTRODUCTION

Recently, the detection of multiferroicity in the $S=1/2$ spin-chain compounds LiCu$_2$O$_2$ (Ref. [1]) and LiCuVO$_4$ (Refs. [2] and [3]) linked together two active research areas of condensed matter physics, namely, multiferroicity and quantum spin systems. The discovery of ferroelectricity (FE) in spiral magnets has strongly revived the field of multiferroicity (see Refs. [4–8], and references therein). In these compounds, complex spin order, which arises from frustrated and competing interactions, is established at low temperatures and induces ferroelectricity. While there is no generally accepted microscopic mechanism for the generation of FE in multiferroics, a number of models providing fundamental and plausible explanations have been developed.[9–13] In most of these systems, e.g., in the rare-earth manganites such as TbMnO$_3$, DyMnO$_3$,[14] TbMn$_2$O$_7$,[15] and Eu:YMnO$_3$,[16] or in Ni$_3$V$_2$O$_8$,[17] FE appears in magnetic phases with spiral or helical order. It has been argued[6] that, qualitatively, these spin structures already break inversion symmetry and FE is induced via spin-orbit coupling. The antisymmetric Dzyaloshinskii–Moriya interaction has been identified as the most likely mechanism prevailing in these materials.[11] A microscopic model based on spin currents in noncollinear magnets has been proposed by Katsura *et al.*[9] Symmetry considerations further reveal that finite polarization P only appears if the vector product of the spiral axis **e** and the propagation vector of spin order **Q** is finite, i.e., $\mathbf{P} \propto \mathbf{e} \times \mathbf{Q}$.[9,10] This specific prediction follows from general symmetry considerations taking into account that magnetism always breaks time inversion, but ferroelectricity only can evolve when spatial symmetry is broken. In this way, the suppression of polarization by external magnetic fields and the complex (H,T) phase diagram in Ni$_3$V$_2$O$_8$ have been explained in a Landau-like theory for continuous phase transitions.[17]

Frustrated spin-1/2 systems display a rich variety of exotic ground states and have attracted considerable attention during the past decade.[18] The simplest frustrated model systems probably are $S=1/2$ spin chains with competing nearest (J_1) and next-nearest (J_2) neighbor interactions. A $T=0$ K, a phase diagram for a $S=1/2$ quantum spin chain with competing J_1 and J_2 exchange has been calculated by Bursill *et al.*,[19] resulting in a spiral spin order with a pitch angle depending on the ratio of J_2 and J_1 for a wide range of parameters. Two prominent examples of quantum spin chains, namely, LiCu$_2$O$_2$ (Ref. [20]) and LiCuVO$_4$,[21,22] indeed, reveal a spiral spin order at low temperatures. With the onset of the complex magnetic order, electrical polarization also emerges in both systems,[1–3] which therefore can be assigned as multiferroic $S=1/2$ quantum spin chains.

In this paper, we study the evolution of ferroelectric polarization in LiCuVO$_4$ as a function of external magnetic fields. In this quantum spin chain, the spiral axis can easily be switched[23] by a magnetic field and, finally, the spiral structure can be completely suppressed,[23,24] which should allow for significant tests of the above-mentioned symmetry considerations.[9,10] However, recently, Moskvin and Drechsler[13] proposed that FE in LiCuVO$_4$ is induced by disorder, which in lowest order generates polarization with **P**∥**a** only. In addition, from detailed electron-spin resonance (ESR) experiments,[25] it has been concluded that, at least in the paramagnetic phase, the antisymmetric Dzyaloshinskii–Moriya interaction plays no role in the magnetic exchange of LiCuVO$_4$. Therefore, a detailed study of the dielectric properties as function of magnetic field seems necessary to construct realistic microscopic models for spiral magnets.

LiCuVO$_4$ crystallizes within an orthorhombically distorted inverse spinel structure. The nonmagnetic V^{5+} ions occupy the tetrahedrally coordinated A sites, while Li$^+$ and Cu^{2+} ($3d^9$ configuration, $S=1/2$) occupy the B positions within the oxygen octahedra of the spinel structure in a fully ordered way. The orthorhombic distortion results from a cooperative Jahn–Teller effect of the Cu^{2+} ions at the octahedral sites. The CuO$_6$ octahedra form independent and infinite chains along the **b** direction, leading to two nearly rectangular Cu-O-Cu superexchange paths between nearest neighbor

(NN) copper ions.[26] There is growing experimental and theoretical evidence that the title compound behaves like a one-dimensional $S=1/2$ Heisenberg antiferromagnet, although details of the next-nearest neighbor (NNN) exchange remain to be clarified.[25,27–30] Magnetic susceptibility, nuclear magnetic resonance (NMR), and ESR experiments revealed an average exchange coupling constant $J \sim 42$ K.[27,29] From neutron diffraction, long-range magnetic ordering with a propagation vector $\mathbf{Q}=(0,0.53,0)$ has been observed below 2.1 K.[21] The incommensurate magnetic order is characterized by Cu^{2+} moments that lie within the **ab** plane with a pitch angle close to 90° and an ordered moment of $0.31\mu_B$. The dispersion of the magnetic excitations has been measured by inelastic neutron scattering.[22] A detailed analysis allowed the determination of the relevant exchange paths resulting in NN ferromagnetic exchange ($J_1 \approx -19$ K), which is active via the two 90° Cu-O-Cu bonds and NNN antiferromagnetic exchange ($J_2 \approx 45$ K) acting via Cu-O-O-Cu superexchange paths. By using quantum spin models,[19] these parameters define a spiral spin ground state with a pitch angle close to 90°, as experimentally observed. A classical Hamiltonian would result in a much smaller turn angle between neighboring spins along the chain. This fact has been taken as proof of the importance of quantum fluctuations in $LiCuVO_4$.[22]

II. EXPERIMENTAL DETAILS

$LiCuVO_4$ single crystals have been prepared as described in detail in Ref. 31. They crystallize in the space group *Imma* and reveal a transition to long-range magnetic order at T_N =2.5 K. They had typical sizes of $3 \times 3 \times 1$ mm³ and were oriented by Laue diffraction. The single crystals used in this work have been characterized by magnetic susceptibility, NMR, and antiferromagnetic resonance techniques.[23] Special care has been taken to choose crystals with almost ideal Li and Cu sublattices. NMR spectra were taken to exclude samples with a non-negligible amount of lithium and copper site disorder.[23] The dielectric measurements were performed for electrical field directions along the three crystallographic axes. For this purpose, silver paint contacts were applied to the platelike single crystals, either in sandwich geometry or by covering two opposite ends of the sample in a "caplike" fashion, therefore leaving a small rectangular gap. The complex dielectric constant was measured for frequencies between 320 Hz and 10 kHz by using an Andeen-Hagerling AH2700A high-precision capacitance bridge. For measurements between 1.5 and 300 K and in external magnetic fields up to 10 T, a Quantum Design Physical Property Measurement System and an Oxford cryomagnet equipped with a superconducting magnet were used. To probe ferroelectric order, we measured both the pyroelectric current at fixed magnetic field H and the magnetoelectric current at fixed temperature by using a high-precision electrometer. The current was integrated to determine the spontaneous polarization. To align the ferroelectric domains when cooling the sample through the transition temperature, we applied a polarizing field of the order of 1 kV/cm.
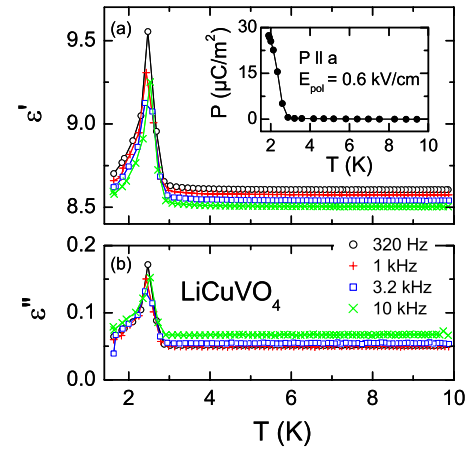

FIG. 1. (Color online) Temperature dependence of the (a) dielectric constant and (b) loss of $LiCuVO_4$ at $T \leq 10$ K for four frequencies with $\mathbf{E} \parallel \mathbf{a}$. The inset shows the temperature dependent polarization along the **a** direction, measured after polarizing the sample during cooling with an electric field of 0.6 kV/cm.

III. RESULTS AND DISCUSSION

Figure 1 shows the temperature dependence of the complex dielectric constant as measured for frequencies between 320 Hz and 10 kHz. The upper frame [Fig. 1(a)] documents the real part of the dielectric constant $\varepsilon'(T)$ around the antiferromagnetic phase transition, the lower frame [Fig. 1(b)] the dielectric loss $\varepsilon''(T)$. These experiments have been performed with the electric field **E** directed along the crystallographic **a** direction. Real and imaginary parts have very similar shapes with a steep rise below 2.8 K, a maximum close to 2.5 K, which corresponds to the magnetic phase transition, and a somewhat smoother decrease toward low temperatures. The peak in ε' signals a transition into a ferroelectric state. Neither ε' nor ε'' reveal any significant frequency dependence. This seems natural, as $LiCuVO_4$ certainly has to be characterized as an improper ferroelectric, where long-range polar order is induced by the onset of a spiral spin order. Hence, no slowing down of polar relaxations is expected. These results are consistent with those published in Refs. 2 and 3, which, however, have been obtained at a single frequency only and without providing information on the dielectric loss or the absolute values of ε'. In the inset of Fig. 1(a), we plot the spontaneous electrical polarization. It appears exactly at T_N and increases to values of approximately 30 μC/m² at 1.9 K, similar to the observation reported in Ref. 3. A rough extrapolation of $P(T)$ toward 0 K gives a saturated polarization of approximately 50 μC/m², a value which is by a factor of 2 lower as compared to the polarization in $Ni_3V_2O_8$ (Ref. 17) and by a factor of 10 lower when compared to the rare-earth manganites.[14] It is, however, by a factor of 10 higher when compared to the ferroelectric quantum spin chain $LiCu_2O_2$.[1] It is interesting to compare the temperature dependence of polarization and dielectric constant at the transition temperature with theoretical predictions: Mostovoy[10] derived a square-root behavior of $P(T)$ and a "1/2 law" for $\varepsilon'(T)$, as observed in proper ferroelectrics. By inspecting the measured temperature dependence of
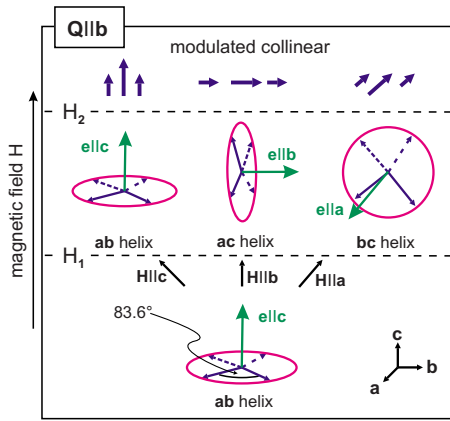
FIG. 2. (Color online) Schematic sketch of the spin configurations as a function of the external magnetic field in magnetically ordered LiCuVO$_4$ ($T < 2$ K) (Ref. 23). H_1 and H_2 indicate phase boundaries between the different magnetic phases. The conelike spin arrangement with a ferromagnetic component in the direction of the normal vector **e**, which likely appears between the fields H_1 and H_2, is not indicated.
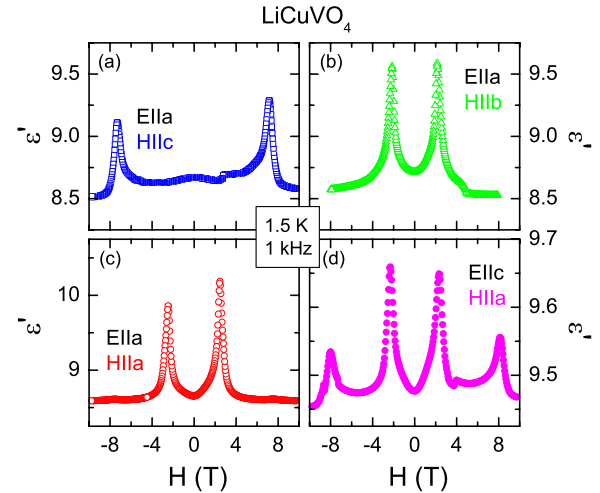

FIG. 3. (Color online) Magnetic-field-dependent dielectric constant of LiCuVO$_4$ at 1 kHz and 1.5 K. The measurements were performed for different directions of electric and magnetic fields as indicated in the figure. All data have been collected by using field sweeps from +10 to −10 T.

the dielectric constant close to T_c (Fig. 1), the spikelike behavior of $\varepsilon'(T)$ seems not to follow $1/(T-T_c)$. However, one should be aware that the ferroelectric anomaly only amounts to approximately 10% of the dielectric constant and any characteristic and critical temperature dependence will be hidden by this large dielectric "background."

The main aim of this work is to follow the dependence of the polarization as a function of the external magnetic field and to check the symmetry relations for spiral magnets as predicted theoretically. In a detailed investigation, Park *et al.*[1] followed the evolution of the polarization $P(T,H)$ in LiCu$_2$O$_2$ along different crystallographic directions in various external magnetic fields. A clear interpretation of the results was hampered by the lack of knowledge about the complex spin configurations as function of temperature and magnetic field. In a previous dielectric work on LiCuVO$_4$,[2,3] the temperature dependence of the capacitance **C** along the crystallographic **a** direction for various magnetic fields was investigated. In addition, the polarization $P(T)$ was measured for various external magnetic fields. However, a systematic study of the magnetodielectric phase diagram of LiCuVO$_4$ is still missing.

Recently, the (T,H) phase diagram of the magnetic phases in LiCuVO$_4$ has been determined by heat capacity, magnetic susceptibility, and high-field magnetization[24] as well as magnetic resonance studies.[23] The deduced spin configurations in the different magnetic states, obtained depending on the external magnetic field at low temperatures, are schematically sketched in Fig. 2. At zero field, these reports find a spin helix within the **ab** plane (**e**∥**c**), with a pitch angle of 83.6° propagating in the **b** direction (**Q**∥**b**). At a critical field H_1 ≈ 2.5 T, the vector **e**, which is orthogonal to the spiral plane, is turned into the direction of the external field. Depending on the direction of this field, the normal vector **e** can point along the crystallographic **a**, **b**, or **c** direction, but the propagation vector **Q** remains unchanged. Finally, above a critical magnetic field H_2, the spiral structure is suppressed. From

combined NMR and ESR experiments,[23] it has been concluded that at high fields, the longitudinal spin component is modulated while the transverse component becomes disordered. We term this partly ordered state "modulated collinear" (see Fig. 2). However, the details of this magnetic structure have to be clarified by neutron scattering experiments. From this phase diagram, it is immediately clear that the polarization should be switchable as a function of the magnetic field and can be fully suppressed for fields $H > H_2$. This seems to be an ideal playground to test the proposed symmetry constraints for spiral magnets as outlined above.

One main result of this investigation is documented in Fig. 3. In zero external magnetic field, **Q**∥**b** holds for the propagation vector and **e**∥**c** for the normal vector of the spiral plane. In spiral magnets where the inverse Dzyaloshinskii–Moriya interaction or spin currents induce the electrical polarization, the polarization **P** is proportional to **e** × **Q**. Accordingly, we expect the ferroelectric polarization to be oriented along **a**, which, indeed, is observed (see Fig. 1). If we apply an external magnetic field along **c**, according to Fig. 2, when H exceeds H_1, the vector **e** will remain parallel to **c** and ferroelectricity with **P**∥**a** is maintained up to H_2, where a collinear structure is established. In this case, we do not expect a phase transition on passing H_1 but probably a spin canting with a concomitant ferromagnetic moment appears, which increases with increasing field. Figure 3(a) showing $\varepsilon'(H)$ measured along **a** for **H**∥**c**, indeed, reveals peaks at about ±7.3 T, i.e., at H_2 and not at H_1. Peaks in ε' are commonly found for ferroelectric transitions and, thus, Fig. 3(a) indicates that FE is stable within these field limits.

If we instead apply the external magnetic field along the crystallographic **b** or **a** direction, at $H > H_1$, ferroelectricity is either completely suppressed (**H**∥**b** → **e**∥**b** → **P** ∝ **e** × **Q** = 0) or the polarization is turned into the **c** direction (**H**∥**a** → **e**∥**a** → **P** ∝ **e** × **Q** ∝ **c**). Indeed, Figs. 3(b) and 3(c) reveal anomalies at about ±2.3 T, corresponding to the critical field
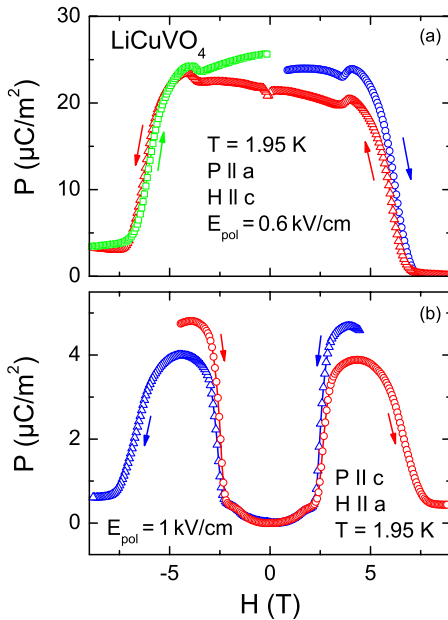
FIG. 4. (Color online) Magnetic-field-dependent electrical polarization of LiCuVO$_4$ along the (a) **a** and (b) **c** directions. The measurements were performed at 1.95 K and for poling fields and magnetic-field directions as indicated in the figure. For the measurements in (a), the sample was cooled at 0 T with a subsequent measuring cycle as indicated by the arrows. The data in (b) were determined after cooling the sample with ±4 T.

H_1. Obviously, not only the ferroelectric-paraelectric transition [Fig. 3(b)], but also the mere change of the polarization direction leads to a peak in ε' [Fig. 3(c)]. Now the critical test is a measurement that is sensitive to the polarization along **c** with the external magnetic field along **a**. At zero field, there is no polarization along the **c** direction, because for the spiral vector, **e**∥**c** holds and, thus, **P** ∝ **e** × **Q** is parallel to **a**. However, on increasing field, above H_1, the normal vector of the spiral reorients parallel to the external field **H**∥**a**, yielding **e**∥**a** and a finite polarization along **c**. This ferroelectric state with **P**∥**c** has to break down again at H_2, where a collinear spin structure is established. The experimental results documented in Fig. 3(d), indeed, are fully consistent with these considerations: At about 2.3 T, FE with **P**∥**c** appears and vanishes again close to 8.1 T, with both transitions leading to peaks in ε'. Obviously, for **H**∥**a**, the phase boundary H_2 is shifted to a somewhat higher value (8.1 T) as compared to 7.3 T for **H**∥**c**. This seems to signal a significant anisotropy of **H**$_2$. Reference 10 documents nicely the strong sensitivity of the dielectric properties of ferroelectric magnets to external magnetic fields and provides illustrative examples on how the spiral undergoes a spin-flip transition, becoming conical and, finally, being flipped by 90°.

To further strengthen the validity of these symmetry constraints and to directly document the polarization switching by external magnetic fields, we also measured the magneto-electric current with different combinations of electric and magnetic field directions. Two representative results are documented in Figs. 4(a) and 4(b). Figure 4(a) shows the field dependence (**H**∥**c**) of the polarization along **a**. In this direction, the spiral phase reveals a macroscopic polarization

and this electrical polarization decays when entering into the collinear spin state. At approximately 7.5 T, the spontaneous polarization has decayed completely. The spiral remains unaffected when passing into the intermediate spin state as the external magnetic field conserves the **ab** helix of the spiral state because **H**∥**c** and, thus, **e**∥**c**. In zero external magnetic field, the polarization along the crystallographic **c** direction is zero [Fig. 4(b)]. Increasing the external magnetic field along **a** induces ferroelectricity at ±2.5 T, which vanishes again for $H > 7$ T. In this case, electrical polarization **P**∥**c** is induced for $H > H_1$, because the normal vector of the spiral plane **e** is turned into the magnetic-field direction (**H**∥**a** and **e**∥**a**). The question remains, why in this case is the polarization by about a factor of 6 lower when compared to the cases **P**∥**a** and **H**∥**c**: This striking anisotropy of the polarization in LiCuVO$_4$ is in accord with recent density functional calculations including spin-orbit coupling.[32] In this theory, it has been shown that the ferroelectric polarization essentially originates from the spin-orbit coupling at the Cu sites, which, depending on the spin orientation, can yield an asymmetric electron-density distribution around the oxygen ions. The resulting polarization **P**∥**a** induced by the **ab** helix was calculated to be approximately six times larger than **P**∥**c** for the **bc** helix, which is in very good agreement with our observations. It only seems that the absolute values of the polarization are overestimated roughly by a factor of 4. However, one has to take into account that the measurements presented here were performed at $0.75 T_N$. Note that within the framework of Ref. 32, the experimentally observed polarization is explained in terms of the electronic charge distribution, and ionic displacements seem to play only a minor role. Finally, we have to state that there is a severe discrepancy of our results documented in Fig. 4(b) as compared to Ref. 3, where zero polarization has been reported for **H**∥**a** and **P**∥**c** at 0 T as well as for 4 T. This disagreement remains unexplained.

The question remains to be addressed if the spontaneous polarization observed in LiCuVO$_4$ really signifies a switchable ferroelectric state. A first indication is given by the fact that the sign of the pyrocurrent directly correlates with the direction of the poling field, when cooling through T_c (not shown). Moreover, Fig. 4 documents that the ferroelectric state can be switched by an external magnetic field: It reveals a polarization with **P**∥**a** in zero external magnetic fields and is switched by 90° (**P**∥**c**) under an applied magnetic field along the **a** direction. We also measured hysteresis loops by using a homebuilt Sawyer–Tower circuit. At all temperatures, the $P(E)$ loops are dominated by a strong linear and paraelectric signal, which is in accord with the small dielectric anomaly at T_c superimposed on the paraelectric background seen in Fig. 1. If one corrects $P(E)$ for this linear dielectric susceptibility, for $T < T_c$, hysteresis loops with a saturation polarization of 10 μC/m^2 (at $T \sim 2$ K) are obtained, which is in rough agreement with the polarization determined via the pyrocurrent (inset of Fig. 1). As the nonlinear parts of the dielectric constant are only 10% of the linear contributions, the resulting hysteresis loops are very noisy and not shown here. Quite generally, such a scenario seems to prevail in multiferroic spiral magnets, which is the reason for the nearly complete absence of published hysteresis loops.
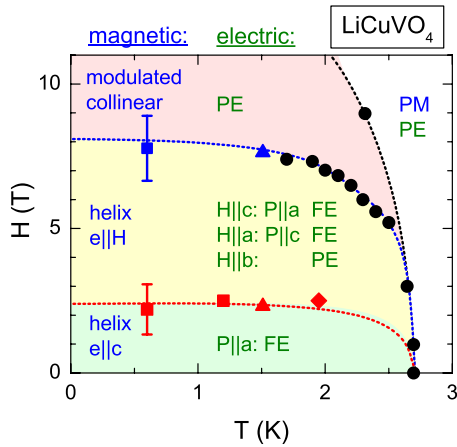
FIG. 5. (Color online) (H,T) phase diagram of LiCuVO$_4$. Results from the present work (triangles and lozenges) and from Refs. 24 (circles) and 23 (squares) were used. The magnetic (left column) and electric states (right column) are noted in the figure.

The results of Figs. 3 and 4 allow the construction of the magnetoelectric (T,H) phase diagram shown in Fig. 5. In addition, results from Refs. 23 and 24 are included. In this schematic phase diagram, we did not take into account the experimentally observed anisotropies of H_2. At low temperatures $(T < T_N \approx 2.5$ K) and at low external magnetic fields $(H < H_1 \approx 2.5$ T), LiCuVO$_4$ reveals a helical spin order with a propagation vector **Q** along **b** and an $(\mathbf{a},\mathbf{b})$ helix (normal vector **e**∥**c**). According to the symmetry rule of spiral magnets, FE is established with the polarization $\mathbf{P} \propto \mathbf{e} \times \mathbf{Q}$ along the crystallographic **a** direction. On increasing magnetic field $(H_1 < H < H_2 \approx 7.5$ T), the normal vector **e** reorients along the external magnetic field and, thus, the electrical polarization depends on the direction of the magnetic field. In this regime, the polarization can be switched from **a** to **c** direction by turning the magnetic field from **c** to **a** direction. In these spin structures with **e**∥**H**, the propagation vector essen-

tially remains the same as for $H < H_1$, i.e., **Q**∥**b**. Hence, when the external magnetic field is along the crystallographic **b** direction, i.e., parallel to the propagation vector, LiCuVO$_4$ is paraelectric. Finally, for external magnetic fields above H_2, the helical spin structure is destroyed and the system is paraelectric for all field directions.

IV. SUMMARY

In summary, we have performed a thorough characterization of the magnetocapacitive properties of multiferroic LiCuVO$_4$ by investigating the dielectric and polarization properties as functions of temperature, magnetic-field strength, and field direction. We construct a detailed (H,T) phase diagram of this prototypical spiral-magnetic multiferroic. At 2.5 K, this $S=1/2$ quantum spin chain undergoes a transition into a helical spin structure, with the spins rotating within the **ab** plane (normal vector **e**∥**c**) and modulation **Q**∥**b**. At 1.95 K, the polarizability amounts to 30 μC/m^2, which is considerably stronger than the polarization in the second known quantum spin chain LiCu$_2$O$_2$. We detected a considerable anisotropy of the polarization, with the absolute value of **P** strongly dependent on the plane of the spin spiral, which is consistent with recent theoretical predictions.[32] Due to the ability to switch the direction of the **ab** helix in the helical spin-ordered state at $H_1 < H < H_2$, LiCuVO$_4$ is ideally suited to test the theoretically predicted symmetry relations for multiferroic spiral magnets.[9,10,32] The symmetry predictions are similar in all these models and we find excellent agreement with our experimental findings. In addition, the density functional calculations of Ref. 32 predicted a striking anisotropy of the polarization in LiCuVO$_4$, which, indeed, is observed.

*Corresponding author.
  peter.lunkenheimer@physik.uni-augsburg.de
†Present address: Universität zu Köln, II. Physikalisches Institut, 50937 Köln, Germany.
[1] S. Park, Y. J. Choi, C. L. Zhang, and S.-W. Cheong, Phys. Rev. Lett. **98**, 057601 (2007).
[2] Y. Naito, K. Sato, Y. Yasui, Y. Kobayashi, Y. Kobayashi, and M. Sato, J. Phys. Soc. Jpn. **76**, 023708 (2007).
[3] Y. Yasui, Y. Naito, K. Sato, T. Moyoshi, M. Sato, and K. Kakurai, J. Phys. Soc. Jpn. **77**, 023712 (2008).
[4] M. Fiebig, J. Phys. D **38**, R123 (2005).
[5] Y. Tokura, Science **312**, 1481 (2006).
[6] D. I. Khomskii, J. Magn. Magn. Mater. **306**, 1 (2006).
[7] S.-W. Cheong and M. Mostovoy, Nat. Mater. **6**, 13 (2007).
[8] R. Ramesh and N. Spaldin, Nat. Mater. **6**, 21 (2007).
[9] H. Katsura, N. Nagaosa, and A. V. Balatsky, Phys. Rev. Lett. **95**, 057205 (2005).

[10] M. Mostovoy, Phys. Rev. Lett. **96**, 067601 (2006).
[11] I. A. Sergienko and E. Dagotto, Phys. Rev. B **73**, 094434 (2006).
[12] J. J. Betouras, G. Giovannetti, and J. van den Brink, Phys. Rev. Lett. **98**, 257602 (2007).
[13] A. S. Moskvin and S.-L. Drechsler, Europhys. Lett. **81**, 57004 (2008).
[14] T. Kimura, T. Goto, H. Shintani, K. Ishizaka, T. Arima, and Y. Tokura, Nature (London) **426**, 55 (2003).
[15] N. Hur, S. Park, P. A. Sharma, J. S. Ahn, S. Guha, and S. W. Cheong, Nature (London) **429**, 392 (2004).
[16] J. Hemberger, F. Schrettle, A. Pimenov, P. Lunkenheimer, V. Yu. Ivanov, A. A. Mukhin, A. M. Balbashov, and A. Loidl, Phys. Rev. B **75**, 035118 (2007).
[17] G. Lawes, A. B. Harris, T. Kimura, N. Rogado, R. J. Cava, A. Aharony, O. Entin-Wohlman, T. Yildrim, M. Kenzelmann, C. Broholm, and A. P. Ramirez, Phys. Rev. Lett. **95**, 087205 (2005).

[18] M. Hase, I. Terasaki, and K. Uchinokura, Phys. Rev. Lett. **70**, 3651 (1993); M. Isobe and Y. Ueda, J. Phys. Soc. Jpn. **65**, 1178 (1996); M. Matsuda, K. Katsumata, K. M. Kojima, M. Larkin, G. M. Luke, J. Merrin, B. Nachumi, Y. J. Uemura, H. Eisaki, N. Motoyama, S. Uchida, and G. Shirane, Phys. Rev. B **55**, R11953 (1997); R. Nath, A. V. Mahajan, N. Büttgen, C. Kegler, A. Loidl, and J. Bobroff, *ibid.* **71**, 174436 (2005).

[19] R. J. Bursill, G. A. Gehring, D. J. J. Farnell, J. B. Parkinson, C. Zeng, and T. Xiang, J. Phys.: Condens. Matter **7**, 8605 (1995).

[20] T. Masuda, A. Zheludev, A. Bush, M. Markina, and A. Vasiliev, Phys. Rev. Lett. **92**, 177201 (2004); A. A. Gippius, E. N. Morozova, A. S. Moskvin, A. V. Zalessky, A. A. Bush, M. Baenitz, H. Rosner, and S.-L. Drechsler, Phys. Rev. B **70**, 020406(R) (2004).

[21] B. J. Gibson, R. K. Kremer, A. V. Prokofiev, W. Assmus, and G. J. McIntyre, Physica B **350**, 253(E) (2004).

[22] M. Enderele, C. Mukherjee, B. Fåk, R. K. Kremer, J.-M. Broto, H. Rosner, S.-L. Drechsler, J. Richter, J. Malek, A. Prokofiev, W. Assmus, S. Pujol, J.-L. Raggazzoni, H. Rakoto, M. Rheinstädter, and H. M. Rønnow, Europhys. Lett. **70**, 237 (2005).

[23] N. Büttgen, H.-A. Krug von Nidda, L. E. Svistov, L. A. Prozorova, A. Prokofiev, and W. Aszmus, Phys. Rev. B **76**, 014440 (2007).

[24] M. G. Banks, F. Heidrich-Meisner, A. Honecker, H. Rakoto, J.-M. Broto, and R. K. Kremer, J. Phys.: Condens. Matter **19**, 145227 (2007).

[25] H.-A. Krug von Nidda, L. E. Svistov, M. V. Eremin, R. M. Eremina, A. Loidl, V. Kataev, A. Validov, A. Prokofiev, and W. Aßmus, Phys. Rev. B **65**, 134445 (2002).

[26] A. Durif, J. C. Grenier, J. C. Joubert, and T. Q. Duc, Bull. Soc. Fr. Mineral. Cristallogr. **89**, 407 (1966); M. A. Lafontaine, M. Leblanc, and G. Ferey, Acta Crystallogr., Sect. C: Cryst. Struct. Commun. **C45**, 1205 (1989); G. Blasse, J. Phys. Chem. Solids **27**, 612 (1965).

[27] A. N. Vasil'ev, L. A. Ponomarenko, H. Manaka, I. Yamada, M. Isobe, and Y. Ueda, Phys. Rev. B **64**, 024419 (2001).

[28] Ch. Kegler, N. Büttgen, H.-A. Krug von Nidda, A. Krimmel, L. Svistov, B. I. Kochelaev, A. Loidl, A. Prokofiev, and W. Aßmus, Eur. Phys. J. B **22**, 321 (2001).

[29] C. Kegler, N. Büttgen, H.-A. Krug von Nidda, A. Loidl, R. Nath, A. V. Mahajan, A. V. Prokofiev, and W. Aßmus, Phys. Rev. B **73**, 104418 (2006).

[30] T. Tanaka, H. Ishida, M. Matsumoto, and S. Wada, J. Phys. Soc. Jpn. **71**, 308 (2002).

[31] A. V. Prokofiev, D. Wichert, and W. Aßmus, J. Cryst. Growth **220**, 345 (2000); A. V. Prokofiev, I. G. Vasilyeva, and W. Aßmus, *ibid.* **275**, 2009(E) (2005).

[32] H. J. Xiang and M.-H. Whangbo, Phys. Rev. Lett. **99**, 257203 (2007).